2020 IEEE/ASME International Conference on
Advanced Intelligent Mechatronics (AIM), Boston, USA
(Virtual Conference), July 6-9, 2020

Redundant Haptic Interfaces for Enhanced Force Feedback Capability Despite Joint Torque Limits

Ali Torabi, Kourosh Zareinia, Garnette R. Sutherland, Mahdi Tavakoli

***Abstract*— In this paper, an actuator saturation compensation method (ASCM) is proposed to enhances the force feedback capability of a redundant haptic interface (RHI) by leveraging its kinematic redundancy. This method acts in the null-space of the Jacobian matrix of the RHI and distributes the overloaded actuator's torque among the available unsaturated actuators at the joints. This method empowers design engineers to utilize smaller actuators that have lower rotor inertia and friction in the design of new haptic interfaces. This is advantageous because having low apparent inertia and friction is a requisite for truthfully recreating the feeling of moving in free space. By employing ASCM, the required torque for rendering a stiff environment will be optimally distributed among small-capacity actuators that otherwise become saturated. Moreover, manipulability enhancement of the RHI along the direction of the task is proposed as a tertiary objective – the primary objective is force reflection and the secondary objective is actuator saturation compensation. The tertiary objective acts if the primary and secondary objectives are feasible, and the haptic interface still has remaining redundancy. Simulation examples are provided throughout the paper to demonstrate the concept. Also, experimental results with a four degree-of-freedom (Dof) planar haptic interface are reported that verify the practicality of the proposed method.**

I. Introduction

To recreate haptic feedback about an environment that is accessed indirectly rather than touched directly by a user, a haptic interface (HI) displays forces received from a virtual or a robotic proxy (slave) probing the environment. Depending on whether the slave is virtual or robotic, a haptic virtual environment or a haptic teleoperation system is formed. Regardless, as the user utilizes the HI to operate the slave that interacts with the environment, haptic feedback about slave-environment interaction displayed by the HI engages the user's sense of touch and should give transparency (i.e., realism and fidelity) to the interaction [1], [2].

Haptic systems have applications in various domains including medicine, e.g., for surgical training with a virtual slave, telesurgery with a robotic slave, and post-disability rehabilitation with a virtual or robotic slave [3]–[5]. High-fidelity haptic feedback, which is critical to the safety and success of any interaction, requires appropriate HI design and control. It has been shown that haptic feedback can increase the precision of the teleoperated surgery, enhance the natural and intuitive conduct of the operation, increase safety, and reduce trauma [6], [7].

Most of the commercially available HIs have a small workspace and/or small force feedback capability. The main reason is that there is a trade-off between the desirable characteristics of HIs [8]. An HI should ideally have low mass, inertia, and friction properties with high force feedback capability [9], [10]. However, requiring a large workspace with high force feedback capability commonly leads to an HI with large inertia and friction. A possible approach for designing HIs with a large workspace and large force feedback capability that have relatively less inertia is employing kinematically redundant serial haptic interface [11]. A kinematically redundant HI (RHI) has more degrees of freedom (DoF) than required to perform a task in the Cartesian space. The kinematic redundancy allows for joint motions/torques that do not affect the end-effector pose/wrench [12]. These joint motions/torques can be employed to achieve multiple objectives in parallel to the primary objective for the RHI, which is reflecting a desired wrench to the human operator.

In the teleoperation literature, kinematic redundancy is mostly considered for slave robots [13]–[16], and the benefits of having a redundant HI have not been comprehensively explored. To the best of knowledge, the only commercial redundant master interface exists in the surgeon's console of the da Vinci Surgical System (Intuitive Inc., CA, USA) [17]. However, haptic feedback is not provided in the da Vinci system. To extend the workspace of HIs, a few researchers have utilized kinematic redundancy [11], [18]–[21]. Teleoperation of a redundant slave robot with an RHI with the same number of DOFs was investigated in [22].

Recently, from our group, Torabi *et al*. [23] showed that by adding one or more DoFs to the base of a non-redundant HI (NHI) to make it an RHI, the workspace and manipulability will be increased while the apparent inertia will be decreased. This implies that the apparent inertia of the RHI in an arbitrary direction is intrinsically smaller than that of the NHI. Also, another intrinsic advantage of the RHI over NHI is its larger effective manipulability. This means that the user needs to move the joints of the RHI less than the joints of the NHI for the same Cartesian-space movement. Therefore, the RHI could display forces to the user with higher fidelity than the NHI. Yet, the force feedback capability of the

* This research was supported in part by the Canada Foundation for Innovation under Grant LOF 28241, in part by the Alberta Innovation and Advanced Education Ministry through Small Equipment under Grant RCP-12-021, in part by the Natural Science and Engineering Research Council of Canada through the Collaborative Health Research Projects, and in part by the Quanser, Inc

A. Torabi and M. Tavakoli are with the Department of Electrical and Computer Engineering, University of Alberta, Edmonton, AB, Canada. {ali.torabi, mahdi.tavakoli}@ualberta.ca

K. Zareinia is with the Department of Mechanical Engineering, Ryerson University, Toronto, Canada. kourosh.zareinia@ryerson.ca

G. Sutherland is with the Project neuroArm, Faculty of Medicine, University of Calgary, Calgary, AB, Canada. garnette@ucalgary.ca

resulting RHI will be upper bounded by that of the NHI. One of the immediate ways to increase the force feedback capability is to use larger actuators and/or gearboxes with higher gear ratios at the joints, both of which will increase the apparent inertia of the RHI and may make it less back-drivable, which is not desirable. An alternative solution to this problem, which is addressed in this research, is employing small actuators that have low rotor inertia and friction in a kinematically redundant serial haptic interface design. We propose to leverage the redundancy of the RHI and re-distribute the torque of overloaded joint's actuator (hereafter called actuator) among the available unsaturated actuators to enhance the force feedback capability of the RHI. This approach will enable the RHI to both have high fidelity and be useful for rendering a wide range of contacts form soft contacts such as brain tissue to hard contacts such as bones.

The inverse kinematic problem of an RHI has an infinite number of solutions [24]. This implies that the RHI can be reconfigured using a null-space controller in many different ways to have a specific posture. Kinematic redundancy can be resolved at velocity, acceleration, or force/torque levels [25]. For the redundancy resolution, the null-space control is often performed with the aim of achieving an objective in parallel to the primary task such as actuator torque limit avoidance [26], [27]. However, this approach does not provide a remedy once an actuator does reach its torque limit [28], [29]. It is actually very common in rendering an environment for the user that one or more of the HI's actuators become saturated as relatively small actuators without gear-head are used in the design of HIs to minimize the inertia and maintain the device's back-drivability [30]. Unlike the NHIs, the actuator saturation problem for the RHIs can be evaded by manipulating the redundancy to distribute the torque among the unsaturated actuators. In a case where one or more actuators are overloaded, a suitable torque command in the null-space of the Jacobian matrix can distribute torque among the unsaturated joints such that the desired force/torque feedback can be provided for the user.

In this research, an actuator saturation compensation method (ASCM) is proposed as a secondary objective in the null space of an RHI. This method enhances the force feedback capability of the RHI by leveraging the kinematic redundancy of the haptic interface and distributing the overloaded actuator's torque among the available unsaturated actuators. This method handles the joint torque bounds of the RHI by successively relieving the joints that exceed their limits when providing force feedback for the user (primary objective). The ASCM addresses the RHI's limitations due to its effective distribution of a desired end-effector Cartesian wrench to joints torque. This method distributes torque among the RHI's actuators as much as possible via the null-space of the RHI until the desired force feedback is not feasible for the RHI. Then, a scaling factor less than unity will be incorporated to downscale the desired force feedback. Furthermore, if after resolving all of the actuator limits, the RHI has any redundancy left, a tertiary objective will be achieved in the null-space of the robotic system to enhance the RHI manipulability.

We discuss how appropriately manipulating an RHI's extra DoFs in joint-level control can enhance its force feedback capability and deal with saturation for small-capacity actuators that bring advantages such as low rotor inertia and friction. This is an effective way to address the trade-offs between the conflicting requirements of a haptic interface, e.g., having large force feedback capability to transparently recreate contact with stiff environments while having low apparent inertia and friction for transparently recreating the feeling of moving in free space. By employing the proposed method, a redundant haptic interface is able to generate larger force feedback with relatively smaller actuators. This feature, in addition to the potential to achieve a tertiary objective, motivates the widespread deployment and utilization of redundant haptic interfaces in the teleoperation context.

The primary task is to reflect force feedback to the user. In Section II, a task-space impedance control as the primary task is developed. As the RHI's actuators have limited capacity, for the case of hard contact, the actuators might become saturated. In this case, the secondary objective, i.e., ASCM, will be activated in order to distribute the overloaded actuators' torque among the available unsaturated actuators. In Section III, the actuator saturation compensation method in the null space of the RHI is proposed. Then, if the system has remaining redundancy after the primary task and the secondary objective are fulfilled, the manipulability of the manipulator can be enhanced along the direction of the task via the tertiary control objective, which is developed in Section IV. In Section V, the experimental results are reported to verify the practicality of the proposed control strategy. Concluding remarks appear in Section VI.

II. Cartesian Space Primary Task Control: End-Effector Impedance Control

Consider a redundant haptic interface in an m-dimensional Cartesian space X with an n-dimensional vector of joint variables q whose task space dynamics can be represented as

$$M_x\ddot{X} + C_x\dot{X} + G_x + F_x = F_m + F_h \tag{1}$$

where $M_x = (JM_q^{-1}J^T)^{-1}$ is the $m \times m$ end-effector inertia matrix or apparent inertia, $C_x = M_x(JM_q^{-1}C_q - \dot{J})J^{\#}$ is the $m \times m$ end-effector's centrifugal and Coriolis forces/torques (wrench) matrix. G_x and F_x are $m \times 1$ vectors of gravitational and friction wrench, respectively, reflected at the end-effector. $J \in \mathbb{R}^{m\times n}$ is the Jacobian matrix and $J^{\#}$ is the generalized inverse of it, defined as $J^{\#} = M_q^{-1}J^T[JM_q^{-1}J^T]^{-1}$ [31]. $F_m = {J^{\#}}^T\tau_m$ is the $m \times 1$ Cartesian-space control wrench vector in which τ_m is the $n \times 1$ joint-level control wrench vector. F_h is the wrench applied by the user's hand on the haptic interface. $M_q(q) \in \mathbb{R}^{n\times n}$ and $C_q(q, \dot{q}) \in \mathbb{R}^{n\times n}$ are joint-level inertia matrix and Coriolis and centrifugal matrix, respectively.

For an RHI, the goal is to generate appropriate control signals, regardless of the operator and environment dynam-

ics, to reflect wrench measured at the environment side (be it virtual or physical) to the operator. Given the end-effector dynamics (1), the Cartesian-space control law is designed as

$$F_m = -F_e - B^d\dot{X} + C_x\dot{X} + G_x + F_x \tag{2}$$

where F_e is the vector of the wrench, which is applied by the environment, and B^d is the desired damping matrix, which is positive definite.

The control law (2) imposes the dynamics of the RHI as

$$M_x\ddot{X} + B^d\dot{X} = F_h - F_e. \tag{3}$$

In the RHI's modified dynamics (3), the operator can smoothly control the desired position, velocity, and acceleration by applying the appropriate force F_h on the end-effector of the RHI. Since the acceleration and velocity are not too large in common operations, the left side of (3) becomes small if the values for the impedance parameters M_x and B^d are sufficiently small. Accordingly, the right side of (3) becomes small ($F_h - F_e \to 0$). Thus, the wrench reflection performance is achieved. If the human operator or the environment applies sudden large forces that generate large acceleration and velocity, the force tracking error at the right side of (3) increases. We are aware that by using slightly more complicated Cartesian space control law, the apparent inertia of the RHI can also be altered [32]. However, if the apparent inertia is reduced less than a specific threshold, the RHI becomes unstable because of losing its passivity [33]. Also, for such a control law, the applied wrench by the user F_h on the HI is also required. Therefore the apparent inertia is kept unchanged in this paper. Also, The HIs are typically designed lightweight and cable-driven, thus, their dynamics have more significant joint friction terms compared to inertia term.

In practice, Cartesian-space control law (2) needs to be implemented in the joint-level. Thus, the corresponding joint-level torque control law can be calculated as

$$\tau_m = J^T F_m. \tag{4}$$

III. Joint-Level Secondary Objective: Actuator Saturation Compensation

A drawback of control law (4), which limits its application for the RHIs, is that joint-level torque limits are not explicitly taken into account. The underlying assumption is that the actuators' capabilities are unlimited, or the robot task has been tailored to fit within the interface's capabilities. However, during interactions between a user and an RHI, it is likely to require large instantaneous joints torque in response to an unexpected situation, e.g., contacting with a solid object. In this section, a method for resolving the torque saturation problem in the joint level is proposed.

Assumption: The underlying assumption in this paper is that the RHI's joints are not at the physical range limit and thus, the end-effector of the RHI is not at the boundary of the workspace. This is because of the fact that when a joint is at its physical limit, the torque saturation level for the joint will be changed from its maximum/minimum level to $\pm\infty$.

For an RHI, the joints' torque control law (4) can be modified by leveraging the kinematic redundancy of the RHI through the null-space control as [34]

$$\tau = \tau_m + \underbrace{(I - J^T J^{\#^T})\tau_N}_{\text{Null-space controller}}, \tag{5}$$

where τ_N is a torque vector corresponding the null space controller in the joint level, and it does not create any end-effector wrench. An appropriately designed τ_N can be used to compensate for the joints' overload in τ_m.

Consider an RHI with the bounds on joint torque as $\mathcal{T}_{min,i} \le \tau_i \le \mathcal{T}_{max,i}$, $i = 1 \dots n$. Also, it should be noted that all the joint-level constraints (e.g., velocity and acceleration) should be converted to the joint torque bound. Now, let us consider a case in which the jth joint of the RHI is overloaded, and its corresponding value in τ_m is either larger than $\mathcal{T}_{max,j} > 0$ or smaller than $\mathcal{T}_{min,j} < 0$. The vector τ_N needs to be designed such that it brings back the torque of joint j within the torque bound by distributing the torque among other joints without overloading them. To design τ_N, first, a diagonal selection matrix $\mathcal{S}$ needs to be defined to identify the saturated joints. $\mathcal{S}$ is defined as an $n \times n$ diagonal selection matrix whose diagonal elements specify whether the joints are saturated or not, i.e., if the j element on the $\mathcal{S}$ diagonal is one, the jth joint of the RHI is saturated. Next, τ_s is introduced as the $n \times 1$ saturation torque vector which its jth non-zero element is either equal to $\mathcal{T}_{max,j}$ or $\mathcal{T}_{min,j}$ corresponding to the saturated joint j. Now, the saturated joints can be isolated with the following Jacobian matrix for the isolated system:

$$\hat{J} = J\mathcal{S}, \tag{6}$$

where J is the Jacobian matrix of the RHI. For the isolated system, control law (5) is rewritten as

$$\tau_s = \hat{J}^T F_m + (I - \hat{J}^T \hat{J}^{\#^T})\tau_N. \tag{7}$$

Therefore, τ_N can be calculated as

$$\tau_N = (I_n - \hat{J}^T \hat{J}^{\#^T})^{\#}(\tau_s - \hat{J}^T F_m). \tag{8}$$

With this choice of τ_N, the torque of joint j will be adjusted back to its saturation level and the associated torque shortage will be distributed between the other joints. However, this can overload other joints of the RHI. Thus, this method needs to be repeated iteratively until either there is no overloaded actuator left or the Cartesian space primary task is found to be infeasible. One can inspect the feasibility of control law (4) for the RHI by checking the rank of $J(I_n - \mathcal{S})$ matrix, i.e., how many joints are not saturated. If the rank of this matrix is smaller than the dimension of the Cartesian space m, the Cartesian space control law F_m is not feasible, and it has to be modified to become realizable for the RHI. In this case, we introduce a scaling factor $0 \le \alpha \le 1$ to make control law (2) realizable. α is equal to one unless the force feedback F_e is not feasible for the RHI. As a result, the control law (2) is modified as

$$\tilde{F}_m = -\alpha F_e + \mu, \tag{9}$$

where

$$\mu = -B^d\dot{X} + C_x\dot{X} + G_x + F_x.$$

Accordingly, the joint-level control vector τ_m needs to be modified to $\tau_m = J^T\tilde{F}_m$. The actuator saturation compensation method (ASCM) calculates the null space control law τ_N, the scaling factor α, and the joint-level control law τ. In this method, first, the most overloaded joint will be identified, and its torque will be adjusted back to the torque saturation limits. Next, the method will look for the new most overloaded joint, if any, to adjust its torque to within the admissible torque limits. This process will be repeated until either there is no overloaded joint remaining or the rank of $J(I_n - \mathcal{S})$ is smaller than the dimension of the Cartesian space. For the latter case, the scaling factor α will be calculated to scale the force feedback and make the control law (5) practical. Algorithm 1 shows the required steps for calculating the scaling factor α.

Algorithm 1 Scaling Factor α Calculation

1: **if** rank$(J(I_n - \mathcal{S})) < m$ **then**
2: $\quad N_0 = (I_n - J^T(J^\#)^T)(I_n - \hat{J}^T\hat{J}^{\#^T})^\#$
3: $\quad N_1 = (-J^T + N_0(JS)^T)F_e$
4: $\quad N_2 = N_0\tau_s + (J^T - N_0(JS)^T)\mu$
5: $\quad \alpha = (\mathcal{T}_{max(min),k} - N_{2,k})/N_{1,k}$
6: $\quad$ ▷ k is the most overloaded joint
7: **end if**

As stated before, one of the advantages of using an RHI over an NHI is that when some of the actuators are overloaded, ASCM saturates them and distributes the remaining torque among the other available (unsaturated) actuators while preserving the direction of the force feedback F_e. However, if this is infeasible, the amplitude of the reflected force is adjusted by $0 \leq \alpha \leq 1$. For the NHI, however, the full capacity of each actuator will not be used and the force feedback amplitude will be much smaller than the desired value in compare to an RHI.

As a simulational example, consider a 3-DoF planar RHI with the links length as $L_i = [0.25,\ 0.25,\ 0.25]\ m$. The joints torque bounds are assumed to be $|\mathcal{T}_i| \leq 0.5$ Nm. The RHI is at $q_i = [\frac{\pi}{4},\ -\frac{\pi}{3},\ -\frac{\pi}{6}]$ rad configuration and supposed to provide environment force feedback to the user when he/she holds the end-effector of the RHI fixed in the task space. The environment force is $F_e = [4\sin(t\pi/2),\ 0]^T$ N, where t is time. Fig. 1 shows the torques of the RHI joints and the output force feedback of the RHI with and without implementing the ASCM. The results show that when a joint is saturated, the ASCM will distribute torque among other joints to provide the desired force feedback by utilizing the full capacity of the RHI's actuators (see Fig. 1(c)). When two joints of the 3 DoF RHI are become saturated, the rank of $J(I_n - \mathcal{S})$ matrix will be smaller than the Cartesian space dimension (2) and from this point, the scaling factor, α, scale the desired force feedback to maintain its direction. When this method is not used, not only the magnitude of desired force feedback cannot be achieved, but also the direction

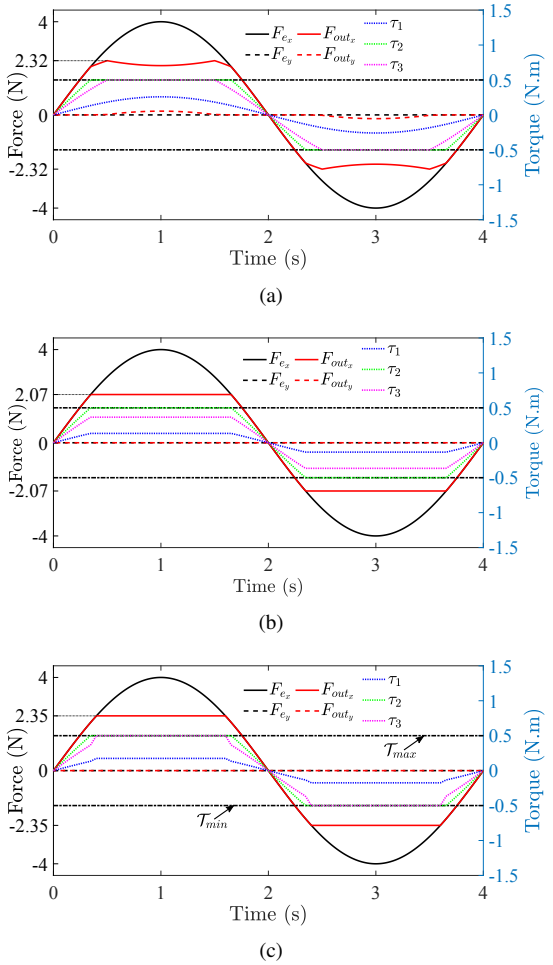

Fig. 1. Joints torque τ_i (dotted lines), desired force feedback F_e (black solid line F_{e_x} and black dashed line F_{e_y}), and output force feedback F_{out} (red solid line F_{out_x} and red dashed line F_{out_y}) of a 3 DoF planar RHI subject to RHI joint saturation. Without any compensation method (a), with simple force feedback scaling algorithm (b), and with the actuator saturation compensation method (c).

of force feedback is altered (Fig. 1(a)). It is noted that a simple scaling method can be used to maintain the direction of the force feedback (Fig. 1(b)), however, in this method, the maximum output force of the RHI is lower than that of the RHI when ASCM is used (12% lower for the 3-DoF RHI example).

IV. Joint Level Tertiary Objective

After the ASCM resolves joint limits, a tertiary objective can be accommodated within the residual torque capacity generation of the RHI. The RHI still has redundant DoF if the rank of $(I_n - \mathcal{S})$ is larger than the dimension of Cartesian space m. Therefore, the RHI is capable of achieving a Tertiary objective by leveraging its redundant joints (i.e., internal motion) without affecting the position and orientation of the end-effector of the robot.

The null-space controller for tertiary objective can be utilized to work in parallel with the primary and secondary tasks controllers. The tertiary objective has a lower priority than the primary and secondary tasks. Therefore, it needs to

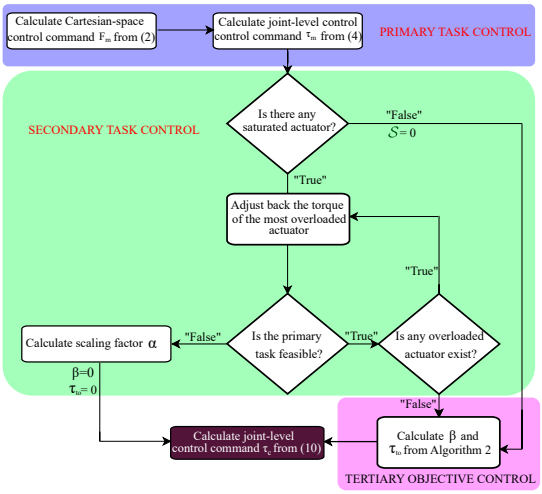

Fig. 2. Flowchart of the control system. It shows the correlation between the primary task (end-effector impedance control), the secondary objective (actuator saturation compensation), and the tertiary objective (manipulability enhancement).

be defined in the null-space of the primary and secondary tasks. In other words, the tertiary objective might not be achieved in favour of realizing the primary task. Also, as the torque limits of the RHI's actuators should not be violated, the ASCM is treated as a secondary task. Therefore, the tertiary objective has to be satisfied in the null space of the ASCM, which has a higher priority than it.

The joint torque command that realizes primary task, ASCM, and a tertiary objective is

$$\tau_C = \tau + \beta(I_n - (\mathcal{S}(I_n - J^T(J^\#)^T))^\#)(I_n - J^T(J^\#)^T)\tau_{to}, \tag{10}$$

where β is the scaling factor to preserve the joint bounds that is between zero and one, τ and $\mathcal{S}$ are calculated from ASCM, and τ_{to} accounts for the tertiary objective. Algorithm 2 shows the required steps for calculating the scaling factor β. This Algorithm calculates the remaining capability of the RHI and determines the scaling factor β according to the joint bounds. If after resolving the joint limits, the RHI does not have any redundant joints left, β will be equal to zero. The flowchart and block diagram of the control system is depicted in Fig. 2 and Fig. 3, respectively.

Algorithm 2 Scaling Factor β Calculation

Get $\mathcal{S}$ from ASCM
if $(I_n - \mathcal{S}) > m$ **then**
  $N_{to} = (I_n - (\mathcal{S}(I_n - J^T(J^\#)^T))^\#)(I_n - J^T(J^\#)^T)$
  $N_3 = N_{to}\tau_{to}$
  $\beta_{min,i} = (\mathcal{T}_{min,i} - \tau_i)/N_{3,i}$ For $i = 1 \rightarrow n$
  $\beta_{max,i} = (\mathcal{T}_{max,i} - \tau_i)/N_{3,i}$ For $i = 1 \rightarrow n$
  Switch $\beta_{min,i}$ and $\beta_{max,i}$ If $\beta_{min,i} > \beta_{max,i}$
  $\beta = \min(\min\{\beta_{max,i}\}, 1)$
else
  $\beta = 0$
end if

There are different methods to implement τ_{to} [24]. Here, the gradient projection approach is used. Thus, the tertiary objective torque is calculated as

$$\tau_{to} = -\Lambda \frac{\partial \nu(q)}{\partial q}, \tag{11}$$

where Λ is a suitable scalar step size and $\nu(q)$ is the cost function. With this choice of τ_{to}, the robot tries to decrease the value of $\nu(q)$ while executing a primary time-varying task. Following the approach introduced in [23], the cost function $\nu(q)$ is selected as

$$\nu = \text{logdet}(\frac{\mathcal{M} + \mathcal{M}^{des}}{2}) - \frac{1}{2}\text{logdet}(\mathcal{M}\mathcal{M}^{des}), \tag{12}$$

where $\mathcal{M}$ is the velocity manipulability ellipsoid of the RHI, defined as $\mathcal{M} = JJ^T$ [35], and $\mathcal{M}^{des}$ is the desired velocity manipulability ellipsoid. By minimizing the cost function (12), the manipulability of the RHI will be matched with the desired one. As shown in [23], by aligning the major axis of the velocity manipulability ellipsoid of an RHI along the desired direction of motion, the reflected joints' friction at the end-effector of the RHI will be minimized, and its manipulability will be maximized. This will consequently minimize the interference of the RHI's kinematic with the perception of the user from the rendered environment. The main limitation of this approach is that the force feedback capability of the RHI along the direction of motion will be minimized due to the fact that the force manipulability ellipsoid is inverse of the velocity manipulability ellipsoid. Therefore, the proposed ASCM is required to distribute torque among the actuators and enhance the force feedback capability of the RHI.

V. Experimental Evaluation

In this section, experiments are performed to evaluate the proposed ASCM and null space controller using a 4-DoF planar RHI. The experiments were performed using a 2-DOF planar upper-limb rehabilitation robot (Quanser Inc., Markham, ON, Canada) that is serially connected to a 2-DoF PHANToM 1.5A (3D Systems Inc., Morrisville, NC, USA) to make the 4-DoF planar RHI. The base joint of the 3-DoF PHANToM robot was removed to turn it into a 2-DoF planar robot. A coupler is designed and 3D-printed to connect the end-effector of the upper-limb rehabilitation robot to the base of the PHANToM robot. To measure forces at the end-effector of the RHI, a 6-DoF force/torque sensor (50M31A3-I25, JR3 Inc., Woodland, CA, USA) is attached to it. The controllers are implemented in MATLAB/Simulink (MathWorks Inc., Natick, MA, USA) with Quarc real-time control software (Quanser Inc., Markham, ON, Canada). The force/torque sensor data are sent through UDP from a Robot Operating System (ROS) PC to the MATLAB PC. The experimental setup is shown in Fig. 4. The joints torque limits are programmed as $\tau_{min,i} = [-3,\ -3,\ -1,\ -1]$ Nm and $\tau_{max,i} = [3,\ 3,\ 1,\ 1]$ Nm, and the links length of the RHI are $d_i = [0.254,\ 0.141,\ 0.21,\ 0.181]$ m.

In the experiments, a user holds the end-effector of the RHI (where the force sensor is shown in Fig. 4) and palpates

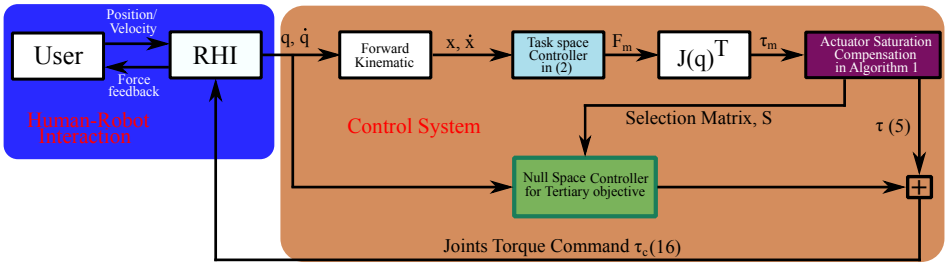

Fig. 3. Block diagram of the control system.

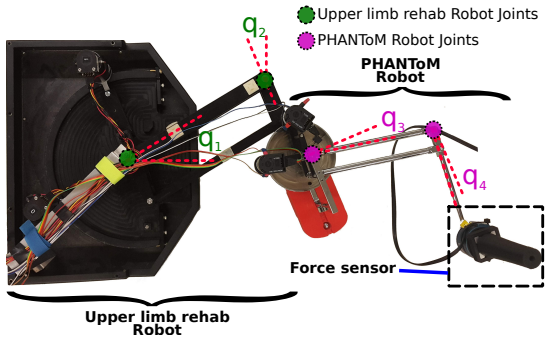

Fig. 4. Top view of experimental setup.

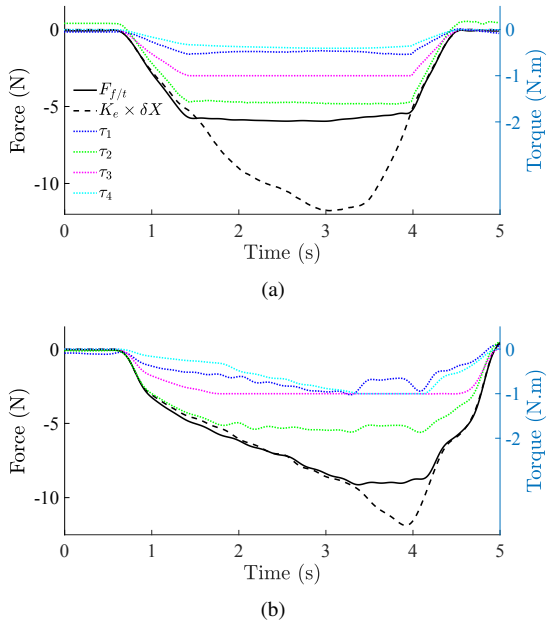

Fig. 5. Experimental results without (a) and with (b) employing the ASCM. Joints torque τ_i, $i = 1, 2, 3, 4$, are shown with dotted lines, desired force feedback $K_e \times \delta X$ with black dashed line, and the measured force feedback $F_{f/t}$ with black solid line.

a virtual environment along the right-hand direction through it. The experiment was approved by the University of Alberta Research Ethics Board under study ID Pro00055825. The virtual environment is modelled as a spring with constant stiffness. In the experiments, the user palpates the virtual environment starting from a fixed point in the workspace of the RHI. The starting point is given as $X_0 = [0.45,\ 0]^T$m. The Cartesian space control law used in the experiments is

$$F_{RHI} = -F_e - B^d\dot{X} + C_x\dot{X} \tag{13}$$

where F_e is modeled as $K_e\delta X$ in which K_e is the stiffness of the virtual environment and δX is the position deviation from the starting point. The desired damping parameter is selected as $B^d = \text{diag}\{0.01,\ 0.01\}$Ns/m. Also, the virtual environment is modelled with $K_e = 1000$ N/m to create a stiff environment. As the end-effector movement is small in the experiment, the effect of friction is neglected, and thus, the friction compensation is not implemented. Also, the gravity compensation is not required as the RHI is planar.

The objective of the experiments is to show the enhanced force feedback capability of the RHI by using the proposed ASCM. Two cases are considered: Case (1) The palpation is performed without the ASCM, and Case (2) The palpation is performed with ASCM. In both cases, the major axis of the desired velocity manipulability ellipsoid is aligned with the direction of motion (contact) (i.e., $u = [0,\ 1]^T$), and it is designed as $\mathcal{M}^{des} = \text{diag}\{0.01,\ 170\}$. The desired velocity manipulability ellipsoid is designed using the method discussed in [23].

Fig. 5 shows the experimental results. In this figure, the measured force using the wrench sensor, the desired force ($K_e \times \delta X$), and the torque of the actuators are illustrated. By employing the ASCM, the maximum force feedback of the RHI is enhanced by 73% (Fig. 5(b)) in comparison to the case in which the palpation is performed without the implementation of ASCM (Fig. 5(a)). The ASCM distributes torque among the unsaturated joints when the saturation happens in one or more joints. As a result, the user feels the environment more solid in case (2).

VI. Concluding Remarks

In this paper, we proposed an actuator saturation compensation method (ASCM) for redundant haptic interfaces that distributes the torque of the saturated joints among the available unsaturated joints. This method leverages the kinematic redundancy of the haptic interface to enable the haptic interface to achieve a higher force feedback capability with relatively smaller actuators. This is important as there is a trade-off between the maximum force feedback capability of the RHI versus minimum apparent inertia and back-drive friction. Indeed, a large force feedback capability requires

large actuators, increasing the haptic interface's inertia. The proposed method generates torque commands in the null-space of the Jacobian matrix of the haptic interface to bring back the overloaded joints to their saturation level and distributes that excessive torque among the unsaturated joints. Also, a tertiary objective null-space controller was proposed that takes the ASCM implementation into account. If the primary task is feasible after ASCM implementation and the redundant haptic interface has available redundancy, a tertiary objective will be satisfied in the null-space of ASCM. This will guarantee that the tertiary objective will not interfere with the primary task and ASCM that those have higher priorities. The experiments with a 4-DoF planar haptic interface demonstrated 73% enhancement in the force feedback capability of the RHI using the proposed methods. The focus of this research is to show that the redundant haptic interface is able to provide larger force feedback to a user with ASCM than without it. Therefore, the method can be used for the design of a new haptic interface with small actuators to provide relatively large force feedback. In the future, we will perform an extensive user study to evaluate how using the proposed method affects the perception of free space and stiff environments.

REFERENCES

[1] K. E. MacLean, "Haptic interaction design for everyday interfaces," *Reviews of Human Factors and Ergonomics*, vol. 4, no. 1, pp. 149–194, 2008.

[2] A. M. Okamura, "Methods for haptic feedback in teleoperated robot-assisted surgery," *Industrial Robot: An International Journal*, vol. 31, no. 6, pp. 499–508, 2004.

[3] M. Kühne, M. Eschelbach, A. Aghaeifar, L. von Pflugk, A. Thielscher, M. Himmelbach, K. Scheffler, P. Smagt van der, and A. Peer, "An mr-compatible haptic interface with seven degrees of freedom," *IEEE/ASME Transactions on Mechatronics*, vol. 23, no. 2, pp. 624–635, April 2018.

[4] M. Shahbazi, S. F. Atashzar, M. Tavakoli, and R. V. Patel, "Robotics-assisted mirror rehabilitation therapy: A therapist-in-the-loop assist-as-needed architecture," *IEEE/ASME Transactions on Mechatronics*, vol. 21, no. 4, pp. 1954–1965, Aug 2016.

[5] B. Hannaford and A. M. Okamura, "Haptics," in *Springer Handbook of Robotics*, B. Siciliano and O. Khatib, Eds. Springer International Publishing, 2016, pp. 1063–1084.

[6] M. Tavakoli, A. Aziminejad, R. Patel, and M. Moallem, "High-fidelity bilateral teleoperation systems and the effect of multimodal haptics," *IEEE Transactions on Systems, Man and Cybernetics – Part B*, vol. 37, no. 6, pp. 1512–1528, December 2007.

[7] T. Yamamoto, N. Abolhassani, S. Jung, A. M. Okamura, and T. N. Judkins, "Augmented reality and haptic interfaces for robot-assisted surgery," *The International Journal of Medical Robotics and Computer Assisted Surgery*, vol. 8, no. 1, pp. 45–56, 2012.

[8] A. Torabi, K. Zareinia, G. R. Sutherland, and M. Tavakoli, "Dynamic reconfiguration of redundant haptic interfaces for rendering soft and hard contacts," *IEEE Transactions on Haptics*, pp. 1–1, 2020.

[9] G. Tholey and J. P. Desai, "A general-purpose 7 dof haptic device: Applications toward robot-assisted surgery," *IEEE/ASME Transactions on Mechatronics*, vol. 12, no. 6, pp. 662–669, Dec 2007.

[10] E. Samur, *Performance metrics for haptic interfaces*. Springer Science & Business Media, 2012.

[11] M. Ueberle, N. Mock, and M. Buss, "VISHARD10, a novel hyper-redundant haptic interface," in *Proceedings - 12th International Symposium on Haptic Interfaces for Virtual Environment and Teleoperator Systems, HAPTICS*, 2004, pp. 58–65.

[12] A. Torabi, M. Khadem, K. Zareinia, G. R. Sutherland, and M. Tavakoli, "Using a redundant user interface in teleoperated surgical systems for task performance enhancement," *Robotica*, p. 1–15, 2020.

[13] D.-Y. Hwang and B. Hannaford, "Teleoperation performance with a kinematically redundant slave robot," *The International Journal of Robotics Research*, vol. 17, no. 6, pp. 579–597, 1998.

[14] A. Zakerimanesh, F. Hashemzadeh, A. Torabi, and M. Tavakoli, "A cooperative paradigm for task-space control of multilateral nonlinear teleoperation with bounded inputs and time-varying delays," *Mechatronics*, vol. 62, p. 102255, 2019.

[15] H. Das, T. B. Sheridan, and J. J. E. Slotine, "Kinematic control and visual display of redundant teleoperators," in *Conference Proceedings., IEEE International Conference on Systems, Man and Cybernetics*, Nov 1989, pp. 1072–1077 vol.3.

[16] P. Malysz and S. Sirouspour, "Trilateral teleoperation control of kinematically redundant robotic manipulators," *The International Journal of Robotics Research*, vol. 30, no. 13, pp. 1643–1664, 2011.

[17] J. K. Salisbury Jr, A. J. Madhani, G. S. Guthart, G. D. Niemeyer, and E. F. Duval, "Master having redundant degrees of freedom," 2004, US Patent 6,684,129.

[18] A. Barrow and W. Harwin, "Design and analysis of a haptic device design for large and fast movements," *Machines*, vol. 4, no. 1, pp. 1–19, 2016.

[19] H. S. Kim, "Kinematically redundant parallel haptic device with large workspace," *International Journal of Advanced Robotic Systems*, vol. 9, no. 6, p. 260, 2012.

[20] F. Gosselin, C. Andriot, F. Bergez, and X. Merlhiot, "Widening 6-dof haptic devices workspace with an additional degree of freedom," in *Second Joint EuroHaptics Conference and Symposium on Haptic Interfaces for Virtual Environment and Teleoperator Systems (WHC'07)*, March 2007, pp. 452–457.

[21] Ö. BAŞER and E. I. Konukseven, "7-dof haptic device and interface design," *Turkish Journal of Electrical Engineering & Computer Sciences*, vol. 21, no. 2, pp. 493–499, 2013.

[22] N. Nath, E. Tatlicioglu, and D. M. Dawson, "Teleoperation with kinematically redundant robot manipulators with sub-task objectives," *Robotica*, vol. 27, pp. 1027–1038, 2009.

[23] A. Torabi, M. Khadem, K. Zareinia, G. R. Sutherland, and M. Tavakoli, "Application of a redundant haptic interface in enhancing soft-tissue stiffness discrimination," *IEEE Robotics and Automation Letters*, vol. 4, no. 2, pp. 1037–1044, April 2019.

[24] B. Siciliano, "Kinematic control of redundant robot manipulators: A tutorial," *Journal of Intelligent and Robotic Systems*, vol. 3, no. 3, pp. 201–212, 1990.

[25] J. Nakanishi, R. Cory, M. Mistry, J. Peters, and S. Schaal, "Operational space control: A theoretical and empirical comparison," *International Journal of Robotics Research*, vol. 27, no. 6, pp. 737–757, 2008.

[26] J. Hollerbach and Ki Suh, "Redundancy resolution of manipulators through torque optimization," *IEEE Journal on Robotics and Automation*, vol. 3, no. 4, pp. 308–316, August 1987.

[27] T.-H. Chen, F.-T. Cheng, Y.-Y. Sun, and M.-H. Hung, "Torque optimization schemes for kinematically redundant manipulators," *Journal of Robotic Systems*, vol. 11, no. 4, pp. 257–269, 1994.

[28] A. Atawnih, D. Papageorgiou, and Z. Doulgeri, "Kinematic control of redundant robots with guaranteed joint limit avoidance," *Robotics and Autonomous Systems*, vol. 79, pp. 122 – 131, 2016.

[29] F. Flacco, A. De Luca, and O. Khatib, "Control of Redundant Robots under Hard Joint Constraints: Saturation in the Null Space," *IEEE Transactions on Robotics*, vol. 31, no. 3, pp. 637–654, 2015.

[30] L. J. Stocco, S. E. Salcudean, and F. Sassani, "Optimal kinematic design of a haptic pen," *IEEE/ASME Transactions on Mechatronics*, vol. 6, no. 3, pp. 210–220, 2001.

[31] O. Khatib, "Inertial Properties in Robotic Manipulation: An Object Level Framework," *International Journal Of Robotics Research*, vol. 13, no. 1, pp. 19–36, 1995.

[32] F. Ficuciello, L. Villani, and B. Siciliano, "Variable impedance control of redundant manipulators for intuitive human – robot physical interaction," *Transactions on Robotics*, vol. 31, no. 4, pp. 1–14, 2015.

[33] J. E. Colgate and N. Hogan, "Robust control of dynamically interacting systems," *International Journal of Control*, vol. 48, no. 1, pp. 65–88, 1988.

[34] O. Khatib, "A unified approach for motion and force control of robot manipulators: The operational space formulation," *IEEE Journal on Robotics and Automation*, vol. 3, no. 1, pp. 43–53, February 1987.

[35] A. Torabi, M. Khadem, K. Zareinia, G. R. Sutherland, and M. Tavakoli, "Manipulability of teleoperated surgical robots with application in design of master/slave manipulators," in *2018 International Symposium on Medical Robotics (ISMR)*, March 2018, pp. 1–6.